Biochimica et Biophysica Acta, 1143 (1993) 273–281

BBABIO 43846

Stark spectra of chlorophylls and carotenoids in antenna pigment-proteins LHC-II and CP-II

Stanisław Krawczyk [a], Zbigniew Krupa [b] and Waldemar Maksymiec [b]

[a] *Institute of Physics and* [b] *Institute of Biology, Division of Plant Physiology, M Curie-Skłodowska University, Lublin (Poland)*

(Received 11 November 1992)

Key words Photosynthesis, Chlorophyll protein, Light-harvesting chlorophyll-protein, LHC-II, CP-II, Spectral form, Stark spectrum

The band structure of low-temperature absorption and Stark spectra of light-harvesting chlorophyll *a/b* protein complexes LHC-II and CP-II is analysed In the red spectral region, the Stark spectrum serves as an independent experimental reference allowing for the resolution of eight bands at 639, 642–3, 649, 656, 662, 665, 671 and 678 nm, consistently with the gaussian deconvolution of the absorption spectrum Different parts of the Stark spectrum are fitted with combinations of the derivatives of either the total absorption spectrum or of individual gaussian components Two electronic transitions at 671 nm and 678 nm and two others at 639 nm and 642–3 nm are found to excite, respectively, localized chlorophyll *a* and chlorophyll *b* states Increased changes in permanent dipole moment, $\Delta\mu \cong 2\,2$ Debye units, corresponding to the transitions at 656 nm and at 665 nm, and an increase in polarizability $\cong 70$ Å^3 corresponding to the first of them indicate that these transitions originate from strong exciton coupling In the violet, the Stark spectra are dominated by the contribution from xanthophylls A value of $\Delta\mu \geq 10$ D was estimated for xanthophyll bands at 484 nm and at 511–513 nm The mechanism of the Stark effect in xanthophylls is briefly discussed

Introduction

The light-harvesting pigment-protein complex LHC-II is the most abundant chlorophyll *a/b* pigment-protein in higher plants and algae, binding more than half of total chlorophylls Recent crystallographic analysis of this complex at 6 Å resolution [1] revealed its structure as a trimer binding 8 molecules of Chl *a* and 7 molecules of Chl *b* in each monomeric unit The chlorophyll molecules are arranged apparently in two layers and intermolecular distances are in the range 9–14 Å, consistent with the high rate of nonradiative energy transfer However, the chlorophylls *a* and *b* were not distinguished from each other, as was also the case for the molecules of xanthophylls

The absorption spectrum of this complex in the red part of the visible spectrum is composed of overlapping bands grouped around two peaks ascribable to Chl *a* (678 nm) and to Chl *b* (650 nm) The analysis of fluorescence polarization data and circular dichroism spectra of a related complex isolated earlier with SDS and called CP-II have led to an approximate model of spatial distribution of pigments [2–4] According to this model, three molecules of Chl *b* interact strongly in a closely spaced symmetric cluster, whereas Chl *a* is deposited more loosely around it Exciton interactions within the Chl *b* trimer result in two degenerate strong transitions at 652 nm and a weaker band at 665 nm, the latter energetically links the Chl *b* energy donors with Chl *a* acceptors, absorbing at 670 and 677 nm Later, new bands were identified and ascribed to Chl *a*-Chl *b* exciton states [5,6]. Picosecond kinetic studies on energy transfer in LHC-II gave different estimates for the transfer time from Chl *b* to Chl *a* (6 ± 4 ps in isolated complex [7] and $0\,5 \pm 0\,2$ ps for LHC-II in situ [8]) Recent measurements revealed the appearance of both picosecond and subpicosecond kinetics [9], consistent with the fast energy transfer between the two chlorophyll species, and in agreement with earlier conclusions based on steady-state polarization measurements [2]

The early model of pigment organization quoted above was originally designed for a pigment system of 3 Chl *a* and 3 Chl *b*, thought to exist in CP-II, actually smaller than that established later for LHC-II, which is

Correspondence to S Krawczyk, Institute of Physics, Maria Curie-Skłodowska University, Radziszewskiego 10, 20-031 Lublin, Poland
Abbreviations Chl, chlorophyll, LHC-II, light-harvesting chlorophyll *a/b* protein associated with Photosystem II, CP-II, light-harvesting chlorophyll *a/b* protein isolated with SDS, SDS, sodium dodecyl sulphate, LD, linear dichroism, CD, circular dichroism

known to consist of 15 pigment molecules This model is based on a simple exciton theory neglecting the possible role of higher excited states and of specific interactions (environmental shifts) in absorption spectra, which turned out to be very important when the problem of band splitting is considered in antenna or reaction center pigment-proteins [10–14] The distribution of pigments within the complex, although as yet approximate, indicates that no pigment clusters can be distinguished [1] A recent study on absorption, CD, LD and fluorescence polarization [15] points to a rather uniform distribution of Chl *b* among Chl *a* and to a complicated structure of the absorption spectrum Thus, the question concerning molecular interactions remains very important and should also include the possible interactions of chlorophylls with carotenoids

In this study, we approach these problems by means of Stark effect spectroscopy, which has an important advantage in that the molecular interactions can be revealed by analysing the Stark spectrum with reference to the absorption spectrum For a single nondegenerate electronic transition in an immobile molecule, the Stark effect (i e , the absorbance change in the external electric field) should be proportional to the second derivative of the absorption spectrum The existence of higher excited electronic states manifests in the admixture of the so-called polarizability term, proportional to the first derivative of absorption, and the general formula describing the Stark spectrum for an isolated molecule has the form [16,17]

$$\Delta A = \frac{(\Delta\mu)^2 F^2}{10\sqrt{2}h^2c^2}[(3\cos^2\delta - 1)\cos^2\chi + 2 - \cos^2\delta]\, D^{(2)} + \frac{\Delta\alpha F^2}{2\sqrt{2}hc}\, D^{(1)} \qquad (1)$$

where

$$D^{(2)} = \nu\frac{d^2(A/\nu)}{d\nu^2} \quad D^{(1)} = \nu\frac{d(A/\nu)}{d\nu}$$

and $\Delta\mu$ is the change in permanent dipole moment on electronic excitation, $\Delta\alpha$ is the polarizability change, F is the electric field strength, δ is the angle between $\Delta\bar{\mu}$ and the transition dipole moment, and χ is the angle between $\bar{F}$ and the electric vector of absorbed light In monomeric Chl *a*, a small but not negligible first-derivative term was found to contribute to the Stark spectra [18], due to mixing of the Q_y transition with Q_x in the electric field This mixing of electronic states leads to a polarizability change $\Delta\alpha$ of several (2–4) Å^3 Strong pigment–pigment interactions in systems with overlapping molecular orbitals involve the charge-transfer transitions and make the Stark bands stronger, this was found to be the case in photosynthetic primary donors in bacteria [19–21] and higher plants [22], and in chlorophyll dimers [18] Also in the case of exciton interactions without orbital overlap, when the electronic excitation is shared by several strongly interacting molecules, theory predicts a strong contribution from the first derivative and from the absorption itself (zeroth derivative) in the Stark spectrum [23] A variety of effects of this kind was found in bacterial light-harvesting pigment-proteins [24,25]

Materials and Methods

LHC-II (light-harvesting chlorophyll *a*/*b* protein of Photosystem II) was isolated and purified from rye by the method of successive cation precipitation as described previously [26] In order to minimize the cation concentration in purified LHC-II, isolates were resuspended and washed three times in 100 mM EDTA (pH 7 7), at a chlorophyll concentration of 0 1 mg/ml Purified LHC-II preparation of at least 95% electrophoretic purity was then resuspended in 50 mM Tricine-NaOH, 100 mM sorbitol buffer (pH 7 8), containing 50% (v/v) glycerol, and stored at −40°C until further use

The corresponding SDS preparation, called usually CP-II, was obtained from 14-day-old bean leaves The chloroplast thylakoids were dissociated for 2 min in 0 3 M Tris-HCl, 1% SDS and 13% glycerol (pH 8 8), and then for 4 min in analogous solution containing 2% sodium deoxycholate instead of SDS Pigment-protein complexes were separated electrophoretically in 0 75 mm polyacrylamide gels according to the procedure described earlier [27] CP-II was usually eluted from the slab and concentrated in 50 mM Tricine (pH 8 0) using an Amicon cell and then immediately used in the experiments In some experiments, slab fragments containing CP-II were used after washing them in 70% glycerol/buffer as described previously [22]

For recording the spectra at low temperatures, the concentration of glycerol in the samples was adjusted to 70% (v/v) The samples were applied to 0 3-mm thick cuvettes with conducting glass windows and frozen in darkness To avoid any cracks in the sample, which is of importance for measuring the electric field induced absorbance changes, the samples were kept at temperatures higher than 77 K

In all experiments described here, the quadratic Stark effect was measured The experimental setup used was as described previously [18,22]

Results

Two kinds of sample were used in the experiments described below The samples were prepared either by adjusting the glycerol content in LHC-II suspension to 70%, or by first adjusting the Triton concentration to a

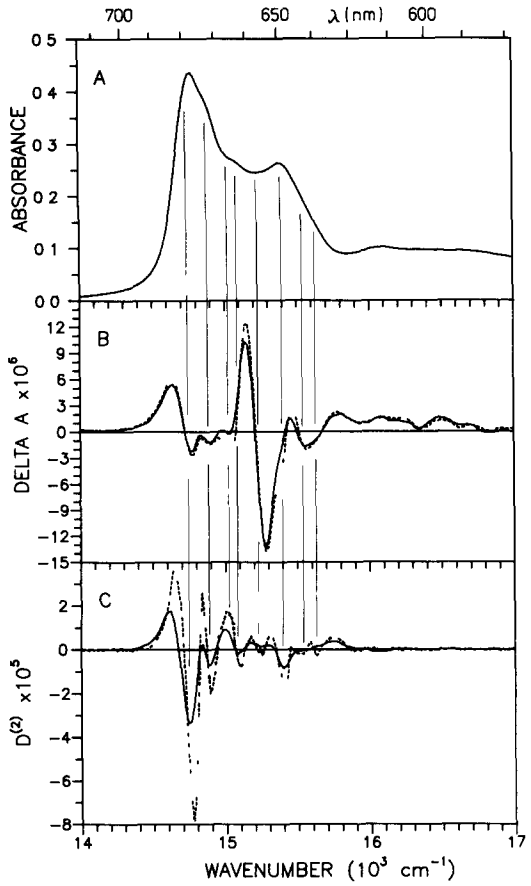

Fig 1 Absorption and Stark spectra of LHC-II in 50 mM Tricine, 100 mM sorbitol, pH 7 8, with 1 mM Triton and 70% (v/v) glycerol Temperature 130 K (A) absorption spectrum (B) Stark spectra at $\chi = 90°$ (continuous line) and $\chi = 54\,7°$ (interrupted line) Electric field strength $F = 8\,82\ 10^4$ V cm^{-1} (rms) (C) the second derivatives of absorption spectra at 130 K (continuous line) and 77 K (interrupted line) The vertical lines indicate the positions of relevant bands in the spectra

value exceeding 1 5–2-times the critical micelle concentration and then adding glycerol after 2–3 min The increased content of Triton in the sample corresponds approximately to the conditions leading to dissociation of aggregated form of LHC-II into trimers [6] Judging by the disappearance of weak light scattering, the dissociation of large aggregates took place before reaching the final Triton concentration No differences were noted on such treatment of LHC-II both in absorption and Stark spectra and in the shape of fluorescence spectra (not reported here)

The absorption spectrum of a LHC-II sample in the region of Q_y transitions in chlorophylls is shown in Fig 1A With the maxima at 677 and at 650 nm and their relative intensities, it is quite analogous to the spectra found in the literature [15,28,29] The corresponding Stark spectrum recorded with the angle $\chi = 90°$ (normal incidence of the light beam onto the sample) is shown in Fig 1B (continuous line) together with the spectrum recorded with $\chi = 54\,7°$ (dashed line) The latter was appropriately scaled with the absorbance ratio so as to compensate for the increase in absorption (and thus in ΔA) on tilting the sample Thus, the differences between these two spectra are directly related to the values of the angle δ (cf Eqn 1) which may be different for different bands

The complex shape of Stark spectra should be compared first of all with the second derivative of the absorption spectrum, represented in Fig 1C The Stark bands, revealed as minima or negative shoulders at 677–8 nm (14 760 cm^{-1}), 671 nm (14 900 cm^{-1}), 649 nm (15 410 cm^{-1}), 642–3 nm (15 560 cm^{-1}) and at 639 nm (15 640 cm^{-1}) have clearly corresponding local minima in the second derivative, except for the Stark band at 665 nm (15 040 cm^{-1}) On the other hand, two bands clearly appearing in the absorption spectrum at 662 nm (15 100 cm^{-1}) and at 656 nm (15 250 cm^{-1}) seemingly are not represented in Stark spectra, but this inconsistency can be due to their overlap with a large bipolar feature centered at 658 nm (15 200 cm^{-1}) All relevant bands found in the red part of the spectrum are listed in Table I

The main feature that makes the Stark spectra different from the second derivative is the inverse proportion of intensities of bands at wavenumbers below 15 000 cm^{-1} corresponding mostly to Chl *a*, and those above 15 000 cm^{-1} originating from Chl *b* The large variability of the proportions between the Stark and second derivative spectra along the wavenumber axis indicates that the electronic transitions represented in absorption are each characterized by a separate set of molecular parameters determining the intensity of the corresponding band in the Stark spectrum

The calculations performed on spectra in different spectral ranges show that a good fit of the Stark spectrum can be obtained with the linear combination of the first and second derivatives of absorption only in the long-wavelength region The fit obtained with the least squares method in the wavenumber range 14 000–15 000 cm^{-1} is represented by the interrupted line in the lower part of Fig 2, where the points represent the experimental data at normal incidence of light onto the sample The coefficients at the derivatives obtained in this way lead to the following values of molecular parameters common to the region of LHC-II spectrum ascribable to Chl *a*

$\Delta\mu = (0\,95 \pm 0\,1)D$

$\Delta\alpha = (8 \pm 2)$ Å^3

$\delta = (40 \pm 6)$ degrees

Thus, the most important parameters $\Delta\mu$ and $\Delta\alpha$ are not very different from those determined previously for monomeric Chl *a* $\Delta\mu = 1$ D and $\Delta\alpha \cong (2\text{–}4)$ Å^3 [18]

At wavenumbers higher than 15 000 cm^{-1}, the Stark spectrum is dominated by strong signals originating from Chl *b* The trials to fit this part of the spectrum with the derivatives of absorption spectrum were unsuccessful This indicates that, due to the overlap of Chl *a* and Chl *b* bands and because of the possible complex excitonic nature of electronic transitions involved, different coefficients must be used for individual bands The necessity of individual treatment of different transitions is also evident from a conspicuous dependence of the Stark signal at 665 nm (15 040 cm^{-1}) on the angle χ (cf Fig 1B)

In order to provide more insight into molecular interactions, we estimated rough values of electrooptical parameters for the eight bands (2–9 in Table I) by deconvoluting the whole absorption spectrum into gaussian components and then fitting the Stark spectrum with the linear combination of their second derivatives The use of gaussian deconvolution is well substantiated in this case by the fact that both absorption (i e , its second derivative) and Stark spectra provide unambiguous and self-consistent information concerning the set of bands that must be taken into account The starting band positions for the deconvolution were taken from the experimental data as listed in the first two columns in Table I Two additional small bands were included into the fit to account for the long-wavelength tail in the absorption spectrum, they were not taken into account in further calculations The results of the deconvolution are presented in Table I and in Fig 3 Generally, the resulting band positions are very similar to those inferred from experimental data, and the band widths for Q_y transitions agree with the widths for isolated chlorophyll

The least-squares fit of the Stark spectrum with a linear combination of only the second derivatives of gaussian bands 2 to 9 is presented in the upper part of Fig 2 Although all bands resolvable in both absorption and Stark spectra have been acounted for, the quality of the fit is rather poor An essential improvement is obtained by adding the first derivative of the band at 656 nm (No 5 in Table I), consistently with the

TABLE I

Deconvolution results

Band positions as detected in the second derivative ($D^{(2)}$) and Stark spectra of LHC-II, the parameters of individual absorption bands from gaussian deconvolution, and their $\Delta\mu$ values

The bandwidths are one-side 1/e widths n r , band not resolved

No	Band positions		Gaussian parameters			$\Delta\mu$ [b] (debyes)
	$D^{(2)}$ cm^{-1} (nm)	Stark cm^{-1} (nm)	max cm^{-1} (nm)	width cm^{-1}	height [a]	
1	16 100 (621)	n r	16 100 (621)	545	0 101	–
2	15 625 (640)	15 635 (639 5)	15 640 (639 5)	173	0 029	1 4–1 9 (1 4)
3	15 528 (644)	15 565 (642 5)	15 570 (642 2)	132	0 074	1 2–1 7 (1 4)
4	15 408 (649)	15 410 [c] (649)	15 405 (649)	136	0 195	0 9–1 3 (1 1)
5	15 248 (656)	n r [d]	15 245 (656)	124	0 137	1 9–2 7 (2 2) $\Delta\alpha = 70$ Å^3
6	15 100 (662)	n r (662)	15 100	136	0 134	1 4–2 0 (1 7)
7	n r	15 040 (665)	15 035 (665)	126	0 109	2 2 $\delta \cong 25°$
8	14 903 (671)	14 900 (671)	14 895 (671 3)	107	0 252	1 1–1 5 (1 2)
9	14 747 (678)	14 760 (677 5)	14 750 (678)	113	0 365	0 8–1 1 (0 9)
10	n r	n r	14 600 (685)	133	0 054	–
11	n r	n r	14 397 (695)	273	0 023	–

[a] Refers to the absorbance spectrum in Fig 1A
[b] Estimate based on the gaussian deconvolution
[c] Shoulder
[d] Dominated by the first derivative

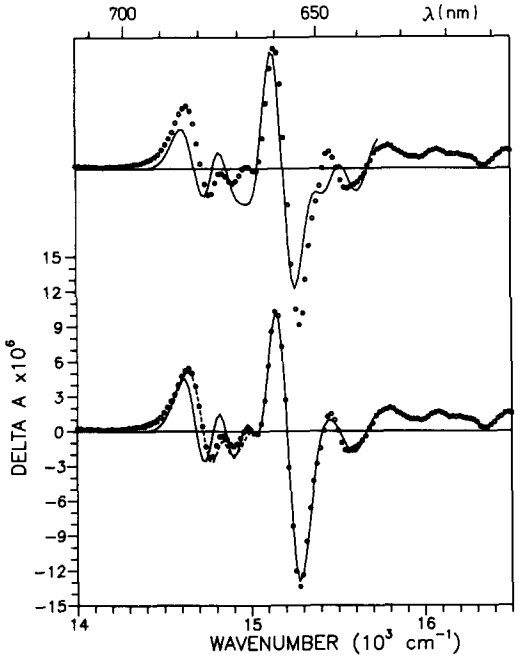

Fig 2 Fits to the Stark spectrum of LHC-II Experimental data are represented by points Continuous line fits based on the linear combination of the second derivatives of gaussian components (upper part) and with the addition of the first derivative of the 656 nm (15240 cm^{-1}) component (lower part) The interrupted line represents the local fit with the first and second derivatives of the absorption spectrum (see text)

large bipolar feature around this wavelength The fit obtained in this way is presented in the lower part of Fig 2 (continuous line) and the resulting values of $\Delta\mu$ and $\Delta\alpha$ are quoted in the last column in Table I Trials

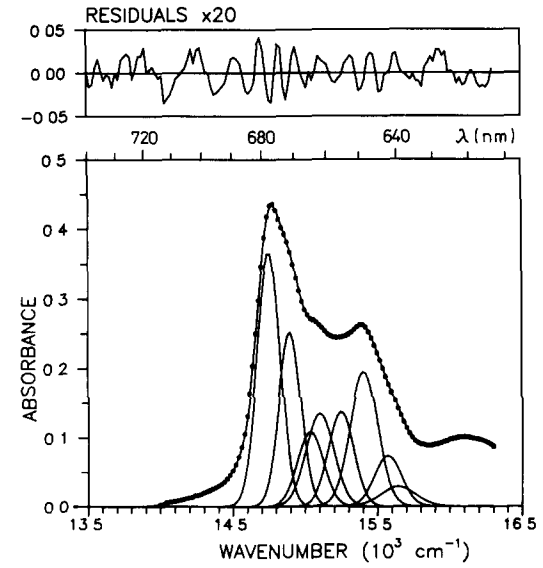

Fig 3 The results of the gaussian deconvolution of the absorption spectrum of LHC-II The parameters of individual components are listed in Table I For clarity, only the components enumerated 2–9 in Table I are shown in this figure

to fit the Stark spectrum by including the first derivatives of other single components did not result in further improvement and often produced negative coefficients at the second derivatives which is an unreasonable result (cf Eqn 1) The remaining discrepancy at wavenumbers below 14800 cm^{-1} could be removed by including the weak bands enumerated 10 and 11 in Table 1 These two bands were not included into the fits because they were not resolved experimentally, and their positions and widths are much less certain than the parameters of other bands

The fitting procedure described above clearly distinguishes two bands One of them, at 656 nm (15250 cm^{-1}, No 5 in Table I), is characterized by remarkably larger $\Delta\mu$ and by a large contribution from the first derivative in the Stark spectrum The other band, at 665 nm (15040 cm^{-1}), which is weak and not clearly resolvable in the absorption spectrum, is related to an electronic transition accompanied by a larger $\Delta\mu$ and exhibits a strong dependence of the Stark signal on the angle χ

The numbers in the last column in Table I specify the range of $\Delta\mu$ values for individual spectral components The values of $\Delta\mu$ were estimated from Eqn 1 by assuming $\chi = 90°$, which is the case for normal incidence of light onto the sample, and by taking into account the maximum variability range of the factor $[2 - \cos^2\delta]$ (cf Eqn 1) Since most of the observed Stark bands, except for the one at 665 nm (15040 cm^{-1}), exhibit only a small increase on changing χ from 90° to 54 7° (see Fig 1), it was estimated from the Stark spectra that the values of the angle δ fall generally within the range 35–45° The assumption of $\delta = 40°$ results in values of $\Delta\mu$ quoted in parentheses in the last column in Table I We consider them to be the most probable estimates of permanent dipole moment changes accompanying the respective electronic transitions in LHC-II

Data analogous to those obtained with LHC-II were also recorded for the chlorophyll-protein complex CP-II, isolated with the use of SDS The absorption, Stark and second derivative spectra are depicted in Fig 4 Although their shapes are analogous to those for LHC-II, they present a weaker resolution of component bands In particular, the cluster of bands between 640 and 662 nm is not resolvable in the absorption spectrum (see the second derivative in Fig 4C) Also, a new weak band seems to appear at about 660 nm

Because of the less precise data on the number and positions of component bands in the spectra of CP-II, systematic analyses of Stark spectra were not performed Only in the spectral range 14000–15080 cm^{-1} were the derivatives of absorption spectrum found to fit the Stark spectrum with $\Delta\mu \cong 0\,9$ D, $\Delta\alpha \cong (7–10)$ $Å^3$, and $\delta \cong 40°$, in analogy with what has been found for LHC-II

In the higher-energy region 17000–25000 cm^{-1}, the absorption spectrum of LHC-II (Fig 5A) consists of bands originating from Chl *a* (435 nm, 22960 cm^{-1}) and Chl *b* (474 nm, 21090 cm^{-1}) with a clear shoulder from xanthophylls at 484 nm (20660 cm^{-1}) Two weaker shoulders can be detected around 494 nm (20220 cm^{-1}) and 511 nm (19580 cm^{-1}), as indicated by the minima in the second derivative in Fig 5C The Stark spectrum in Fig 5B has several minima generally coincident with the minima in the second derivative This implies a substantial contribution from $\Delta\mu$-based mechanism for the Stark effect in xanthophylls Assuming $\Delta\alpha = 0$, we can estimate the angle δ between $\Delta\mu$ and the electronic transition moment as equal to 16° for the band at 511 nm (513 nm in the second derivative) and about 20–25° for the one at 484 nm (20660 cm^{-1}) A value of $\Delta\mu \cong 8$ D can be estimated for the band at 484 nm directly from the data in Fig 5B and C Application of gaussian deconvolution procedure allows to approximately estimate the $\Delta\mu$'s for both bands at 484 nm and at 511 nm (19580 cm^{-1}) as being at least 10 D

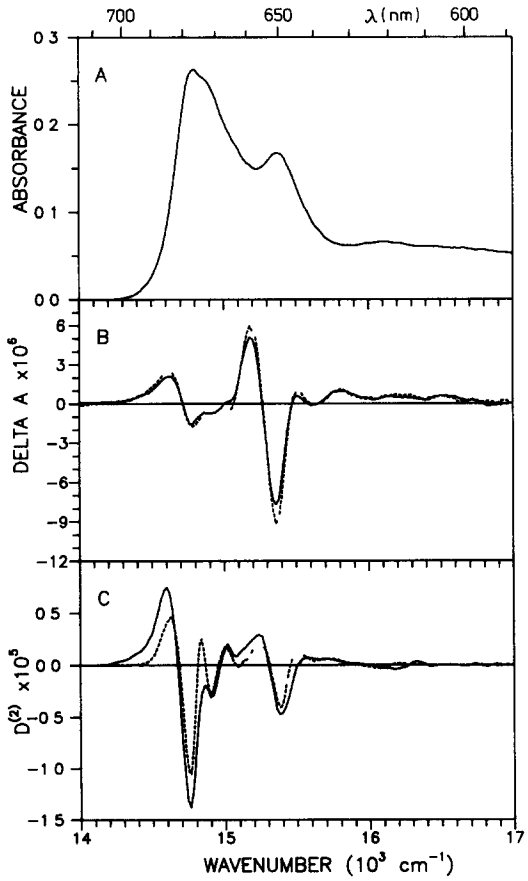

Fig 4 Absorption and Stark spectra of CP-II in 50 mM Tricine buffer, (pH 8 0), with 70% (v/v) glycerol Temperature 142 K (A) Absorption spectrum (B) Stark spectra at $\chi = 90°$ (continuous line) and $\chi = 54\ 7°$ (interrupted line) Electric field strength $F = 8\ 53\ 10^4$ V cm^{-1} (rms) (C) The second derivatives of absorption spectrum at 142 K (continuous line) and at 77 K (interrupted line, divided by 2 5)

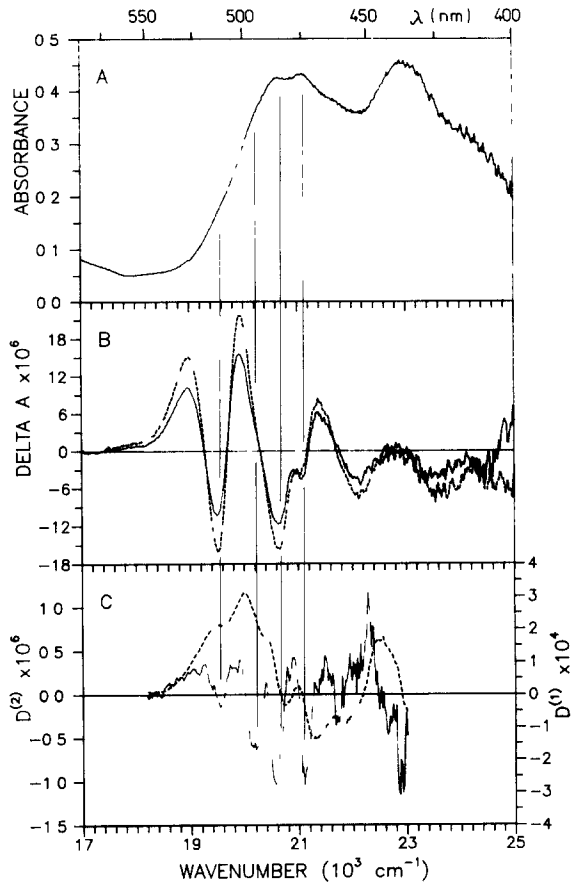

Fig 5 Absorption and Stark spectra of LHC-II Sample conditions, temperature and field strength as in Fig 1 (A) Absorption spectrum (B) Stark spectra at $\chi = 90°$ (continuous line) and $\chi = 54\ 7°$ (interrupted line) (C) the second derivative (continuous line) and the first derivative (interrupted line) of absorption spectrum

The appearance of strong Stark bands from xanthophylls in the range 18000–20000 cm^{-1} suggests that also at higher wavenumbers the Stark spectrum is dominated by the signals originating from xanthophylls Indeed, almost all prominent extrema exhibit a uniform dependence on the angle χ Only one exception can be noted at 21090 cm^{-1}, i e in the maximum of Chl *b* absorption, where the angular dependence of Stark signals appears to be inverse The weakening of the negative signal with the decrease of χ implies that the Stark effect within this band has a significant contribution from the change in permanent dipole moment oriented at an angle $\delta > 54\ 7°$ relative to the transition moment In the case of Chl *a* band at $\cong 23000$ cm^{-1}, no clear conclusion concerning the mechanism of the Stark effect can be drawn because of weaker signals and increased noise in this region

Discussion

The comparison of $\Delta\mu$ for chlorophylls in pigment-protein and in nonpolar solvent would require the local field factor *f*, defined as $f = F/F_{macro}$, to be taken into

account, since only the product $f\ \Delta\mu$ is obtained from experiment An analysis based on expressions for the local field factor [30] shows that the correction factor relating $\Delta\mu$ measured here with that found for chlorophylls in frozen nonpolar solvents lies in the range $f = 1\ 07–1\ 16$, and thus its effects are below the experimental accuracy

For two of the eight individual absorption bands considered, at 678 nm (14760 cm^{-1}) and 671 nm (14900 cm^{-1}), the values of $\Delta\mu$ estimated from the fits of the Stark spectrum by either the derivatives of total absorption or of gaussian components, are in the range $1 \pm 0\ 2$ D, which is close to $\Delta\mu$ for monomeric Chl *a* [18] Moreover, the absorption bands at 678 and 671 nm originate from Chl *a* molecules that can be considered as only weakly coupled to the other ones by transition dipole interaction If the presence of higher excited states is neglected, which is the usual assumption in the weak coupling limit, then the wavefunction of the system of interacting molecules can be written as a linear combination of product wavefunctions, each representing a state with one excited molecule

$$\Psi_k = \sum_i C_{ki}\ \chi_i, \quad \chi_i = \phi_1^0\ \phi_2^0 \quad \phi_i^1 \quad \phi_n^0 \tag{2}$$

where ϕ_m^0 and ϕ_m^1 are the ground and the first excited state of mth molecule, and the set of coefficients C_{ki} is different for each exciton state 'k' In such a case, the change in permanent dipole moment of the system, accompanying the kth exciton transition, is

$$(\Delta\bar{\mu})_k = \sum_i (C_{ki})^2\ \Delta\bar{\mu}_i \tag{3}$$

Since $\Sigma_i (C_{ki})^2 = 1$, it follows from Eqn 3 that for a system of identical molecules with differently oriented $\Delta\bar{\mu}$ vectors, the resultant value of the vector $(\Delta\mu)_k$ shall be not larger than the value of permanent dipole change $\Delta\mu_i$ of an individual molecule Also, the angle δ for an exciton transition can be quite different from its 'monomeric' value Thus, the fact that the permanent dipole moment changes accompanying electronic transitions at 678 nm (14760 cm^{-1}) and 671 nm (14900 cm^{-1}) are quite similar to the values characteristic for monomeric Chl *a*, points strongly to the localized nature of corresponding excited states These states are characterized by a set of expansion coefficients C_{ki}, of which only one is near unity and the remaining ones are nearly zero The highly localized character of electronic excitations corresponding to the absorption of Chl *a* at 678 and 671 nm suggests that the main factor determining the red shift in these spectral forms is the specific physicochemical interaction of Chl *a* molecules with the surrounding medium rather than the exciton splitting

The CD spectra of LHC-II and CP-II are significantly different, generally, the intensity of CD signals in the region of Chl *a* absorption is much smaller in CP-II [3,4] than in LHC-II [6,15] However, there are no such differences in both absorption and Stark spectra of these preparations except for some loss of spectral resolution, possibly related to increased spectral inhomogeneity in CP-II Taken together this means that CD signal at 670–690 nm arises from interactions of Chl *a* molecules weak enough so as not to change the positions of absorption bands or their electrooptical characteristics At the level of experimental accuracy attained in this study, we cannot find the evidence for a strong coupling of Chl *a* absorbing at 671–672 nm with higher-energy states, as suggested in Ref 5

The above arguments emerging from exciton theory can be applied also to the other two Stark bands at 639 nm (15640 cm^{-1}) and 642–3 nm (15560 cm^{-1}), which, judging by their positions in the spectrum, are ascribable to Chl *b* The appearance of a composite band structure at 640–645 nm was not revealed in absorption spectra [28,29] and was recently postulated on the basis of differences in CD and LD spectral features in this region [15] The values of dipole moment changes, $\Delta\mu = 1\ 4–1\ 6$ D, typical for monomeric Chl *b* (Krawczyk, S , unpublished results), point to 'monomeric', i e essentially localized, character of electronic transitions underlying these overlapping absorption bands

The prominent absorption band at 649 nm (15410 cm^{-1}) is represented in the Stark spectrum by only a weak feature appearing as a shoulder at the same wavelength (Fig 1) Also, the other band at 662 nm (15100 cm^{-1}), clearly resolvable in the absorption spectrum (see the second derivative in Fig 1C) is not seen, apparently because of its overlap with the strong bipolar feature centered at 656–8 nm (15240 cm^{-1}) Although the curve fitting procedure used here gives quite reasonable values of $\Delta\mu$ for these two bands (1 1 and 1 7 D, respectively), the reliability of these results is uncertain due to the weakness and overlap of corresponding bands in the Stark spectrum, and we cannot ascribe a particular significance to them

The remaining two electronic transitions giving rise to absorption bands at 656 nm (15240 cm^{-1}) and at 665 nm (15040 cm^{-1}) are both characterized by an increased change in permanent dipole moment, about 2 2 D Additionally, a large increase in polarizability, $\Delta\alpha = 70$ Å^3, accompanies the first transition, while for the second one the vector $\Delta\mu$ is directed close to the transition moment The effective values of $\Delta\mu$ exceeding 2 D and thus larger than those for monomeric Chl *a* or Chl *b*, and other untypical characteristics, indicate that the assumptions underlying Eqn 2 are inapplicable, and the exciton interaction resulting in these electronic transitions is as strong as to mix other electronic states (ground and higher excited) to the electronic wavefunction of the excited state In such a case,

theory predicts a significant admixture of the first- and, possibly, zeroth-derivative terms into the Stark spectrum [23] Due to the limitation imposed by the overlap of individual bands in both absorption and Stark spectra, it is rather difficult to reliably assess the possible polarizability contribution to the Stark band at 665 nm For the same reason the estimates of $\Delta\mu$'s for both these transitions shall not be regarded as to representing their close values but, together with other peculiarities mentioned above, are rather a semiquantitative indication of exciton interaction strong enough to distort the distribution of electronic charge in molecules involved Our conclusion that these effective values of $\Delta\mu$ and $\Delta\alpha$ are related to interactions of the exciton type, and not to more specific physicochemical interactions with, e g , protein, is supported by the appearance of a strong band around 650 nm in CD spectra of both LHC-II [6,15] and CP-II [3,4] The persistence of this exciton feature points to the localization of responsible molecular structure (Chl *b*) in the protein core

The trimeric exciton model [2–4] postulates the existence of two energy levels resulting from strong coupling between three Chl *b* molecules one doubly degenerate, excitable at 652 nm, and the other one which is weaker, at 665 nm The large polarizability change accompanying the 656 nm transition can be indicative of its degeneracy in terms of the trimeric exciton model This electronic state is thought to act as an acceptor of excitation energy from Chl *b*, and the second one, at 665 nm, to transfer the energy to Chl *a* A recent kinetic study [8] confirmed the requirement for a strong coupling between the state excited at $\cong$ 650 nm and some other state of lower energy and with improved overlap with Chl *a* Our data confirm the existence of such excited states corresponding to absorption bands at 656 and 665 nm, resulting from strong exciton coupling in a Chl *b* cluster and energetically linking the mainly localized electronic states of Chl *b* excitable at shorter wavelengths with those of Chl *a* in the long-wavelength part of the LHC-II spectrum This link is probably responsible for the sub-picosecond rates of energy transfer from Chl *b* excited at 650 nm to Chl *a* absorbing at $\cong$ 670 nm and longer wavelengths [8,9], otherwise difficult to reconcile with the weak-coupling Forster theory [8]

As was pointed out in the preceding section, the overall picture in the blue part of the spectrum suggests that the contributions from both chlorophylls to ΔA are rather insignificant, and the Stark spectrum is dominated by signals originating from xanthophylls Despite of the complexity of the overall spectrum, the mechanism of the Stark effect based on the change in permanent dipole moment can be safely ascribed to the electronic transitions in xanthophyll at 484 nm (20 660 cm^{-1}) and to the one at 511–513 nm ($\cong$ 19 580 cm^{-1}), corresponding to $\Delta\mu \geq 10$ D The spacing of these bands, about 1100–1150 cm^{-1}, indicates that both these bands can be attributed to the same xanthophyll species The Stark signal originating from the other xanthophyll and corresponding to the shoulder in absorption at 494 nm (20 220 cm^{-1}) is much weaker, and thus no clear mechanism can be indicated for it Generally, the findings indicating a substantial increase of permanent dipole moment in some xanthophyll species in LHC-II are analogous to what has been observed for carotenoids in bacterial antenna complexes [25]

The xanthophyll content of LHC-II is labile and is known to include lutein, neoxanthin and violaxanthin in the total number of about three [31] to five [32] xanthophylls per 15 chlorophylls in a monomeric unit [33] The assignment of absorption bands to particular xanthophylls has not yet been done In solvents of different polarity, the redmost maxima of absorption are positioned at 472–476 nm for lutein, 464–468 nm for neoxanthin and at 468–471 nm for violaxanthin [34] Of these three xanthophylls only neoxanthin has an asymmetric molecular structure, which may be responsible for a change in permanent dipole on electronic excitation The studies of the Stark effect in lutein [35] showed no appreciable contribution from permanent dipole Thus, the value of $\Delta\mu \geq 10$ D for xanthophyll band at 511–513 nm and its strongly red-shifted position might be attributed to neoxanthin However, neoxanthin is present only in a small proportion to lutein and violaxanthin [31,32,34] On the other hand, the long polyenic chains are highly polarizable [35,36] and thus an internal permanent electric field in the protein may also be operative in inducing significant dipole moment in the symmetric xanthophylls The lack of band assignments to particular xanthophylls makes a definitive explanation difficult at present

In conclusion, our results are the first to confirm directly the strong exciton coupling in a set of a few (two or three) molecules of Chl *b*, which gives rise to electronic states considered to link the higher-energy excited states in Chl *b* with the lower-energy states in Chl *a*, as postulated in the early exciton model of CP-II and LHC-II They point also to significant modifications in the electronic structure of xanthophylls bound to LHC-II

Acknowledgements

This work was financially supported by the Polish Committee for Scientific Research

References

1 Kuhlbrandt, W and Wang, D N (1991) Nature 350, 130–134
2 Van Metter, R L (1977) Biochim Biophys Acta 462, 642–658

3 Shepanski, J F and Knox, R S (1981) Isr J Chem 21, 325–331
4 Gulen, D and Knox, R S (1984) Photobiochem Photobiophys 7, 277–286
5 Gulen, D , Knox, R S and Breton, J (1986) Photosynth Res 9, 13–20
6 Ide, J P , Klug, D R , Kuhlbrandt, W , Giorgi, L B and Porter, G (1987) Biochim Biophys Acta 893, 349–364
7 Gillbro, T , Sundstrom, V , Sandstrom, A , Spangfort, M and Andersson, B (1985) FEBS Lett 193, 267–270
8 Eads, D D , Castner, E W , Jr , Alberte, R S , Mets, L and Fleming, G R (1989) J Phys Chem 93, 8271–8275
9 Kwa, S L S , Groeneveld, F G , Dekker, J P , van Grondelle, R , van Amerongen, H , Lin, S and Struve, W S (1992) Biochim Biophys Acta 1101, 143–146
10 Knapp, E W , Fischer, S F , Zinth, W , Sander, M , Kaiser, W , Deisenhofer, J and Michel, H (1985) Proc Natl Acad Sci USA 82, 8463–8467
11 Eccles, J , Honig, B and Schulten, K (1988) Biophys J 53, 137–144
12 Eccles, J and Honig, B (1983) Proc Natl Acad Sci USA 80, 4959–4962
13 Mar, T and Gingras, G (1984) Biochim Biophys Acta 764, 283–294
14 Scherz, A and Parson, W W (1984) Biochim Biophys Acta 766, 666–678
15 Hemelrijk, P W , Kwa, S L S , van Grondelle, R and Dekker, J P (1992) Biochim Biophys Acta 1098, 159–166
16 Liptay, W (1965) 2 Naturforsch 20 A, 272–289
17 Reich, R and Schmidt, S (1972) Ber Bunsenges Physik Chem 76, 589–598
18 Krawczyk, S (1991) Biochim Biophys Acta 1056, 64–70
19 Lockhart, D J and Boxer, S G (1987) Biochemistry 26, 664–668
20 Losche, M , Feher, G and Okamura, M Y (1987) Proc Natl Acad Sci USA 84, 7537–7541
21 Boxer, S G , Goldstein, R A , Lockhart, D J , Middendorf, T R and Takiff, L (1989) J Phys Chem 93, 8280–8294
22 Krawczyk, S and Maksymiec, W (1991) FEBS Lett 286, 110–112
23 Scherer, P O J and Fischer, S F (1986) Chem Phys Lett 131, 153–159
24 Gottfried, D S , Stocker, J W and Boxer, S G (1991) Biochim Biophys Acta 1059, 63–75
25 Gottfried, D S , Steffen, M A and Boxer, S G (1991) Biochim Biophys Acta 1059, 76–90
26 Krupa, Z , Huner, N P A , Williams, J P , Maissan, E and James, D R (1987) Plant Physiol 84, 19–24
27 Baszyński, T , Tukendorf, A , Ruszkowska, M , Skórzyńska, E and Maksymiec, W (1988) J Plant Physiol 132, 708–713
28 Brown, J S and Schoch, S (1981) Biochim Biophys Acta 636, 201–209
29 Brown, J S (1983) Photosynth Res 4, 375–383
30 Bottcher, C J F (1973) Theory of Electric Polarisation, Vol I, Elsevier, Amsterdam
31 Peter, G F and Thornber, J P (1988) in Photosynthetic Light-Harvesting Systems (Scheer, H and Schneider, S , eds), pp 175–186, W de Gruyter, New York
32 Siefermann-Harms, D (1985) Biochim Biophys Acta 811, 325–355
33 Butler, P J G and Kuhlbrandt, W (198 8) Proc Natl Acad Sci USA 85, 3797–3801
34 Lichtenthaler, H K (1987) Methods Enzymol 148, 350–382
35 Schmidt, S and Reich, R (1972) Ber Bunsenges Physik Chem 76, 1202–1208
36 Liptay, W (1974) in Excited States, Vol I (Lim E C ed), Vol 1, pp 129–229, Academic Press, New York